Electronic Supplementary Material (ESI) for Physical Chemistry Chemical Physics.

Supplementary materials

Novel organic semiconductor based on 2-amino-anthracene: synthesis, charge transporting and photoconductive properties

K. Kondratenko[a*], I. Carlescu[b], P.-E. Danjou[c], Y. Boussoualem[a], A. Simeon[b], B. Duponchel[a], J.F. Blach[d], C. Legrand[a], N. Hurduc[b] and A. Daoudi[a]

[a]Univ. Littoral Côte d'Opale, UR 4476 - UDSMM - Unité de Dynamique et Structure de Matériaux Moléculaires, 59140 Dunkerque, France
[b]Department of Natural and Synthetic Polymers, Faculty of Chemical Engineering and Environmental Protection, “Gheorghe Asachi” Technical University of Iasi, 700050 Iasi, Romania.
[c]Univ. Littoral Côte d'Opale, UR 4492 - UCEIV - Unité de Chimie Environnementale et Interactions sur le Vivant, 59140 Dunkerque, France.
[d]Univ. Artois, CNRS, Centrale Lille, ENSCL, Univ. Lille, UMR 8181, Unité de Catalyse et Chimie du Solide (UCCS), 62300 Lens, France

* Electronic mail: kirill.kondratenko@univ-lille.fr

NMR spectra

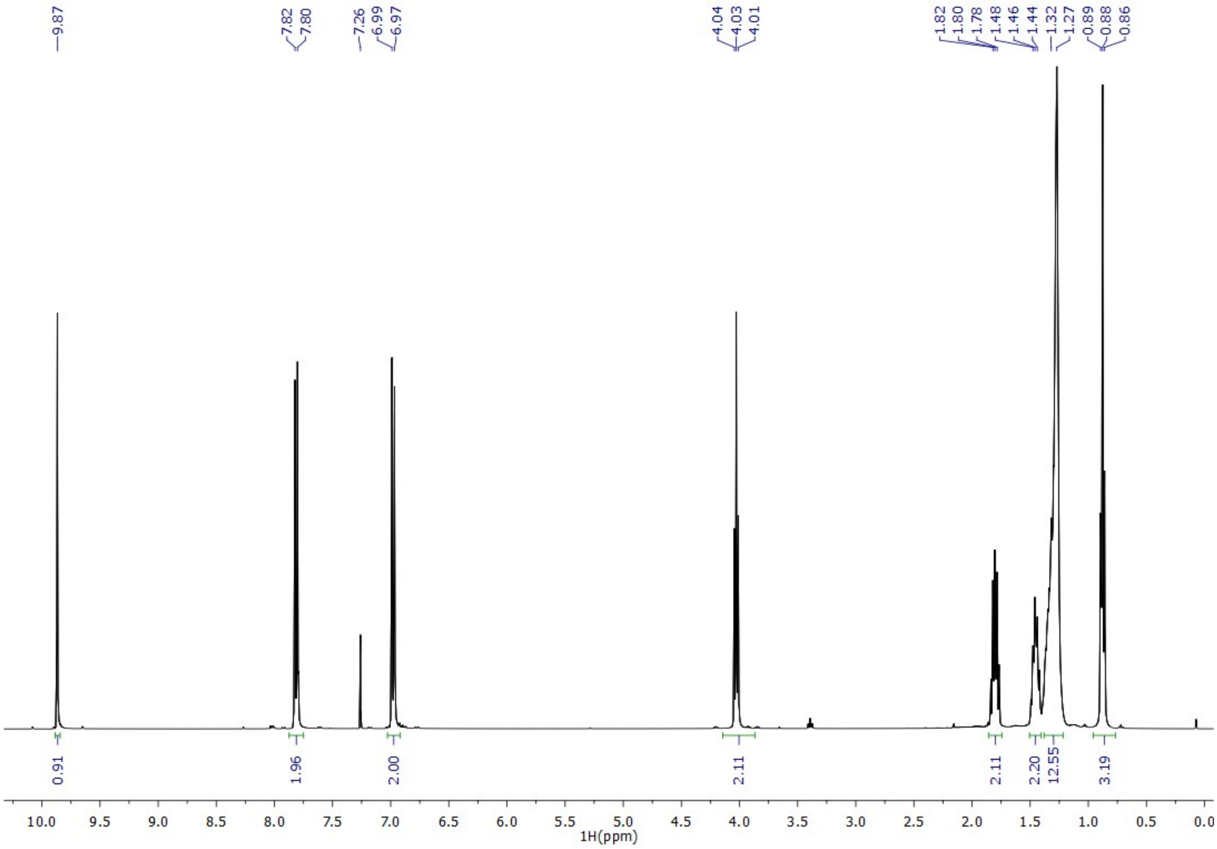

Figure 1. ^1H NMR spectrum of 4-(decyloxy)benzaldehyde.

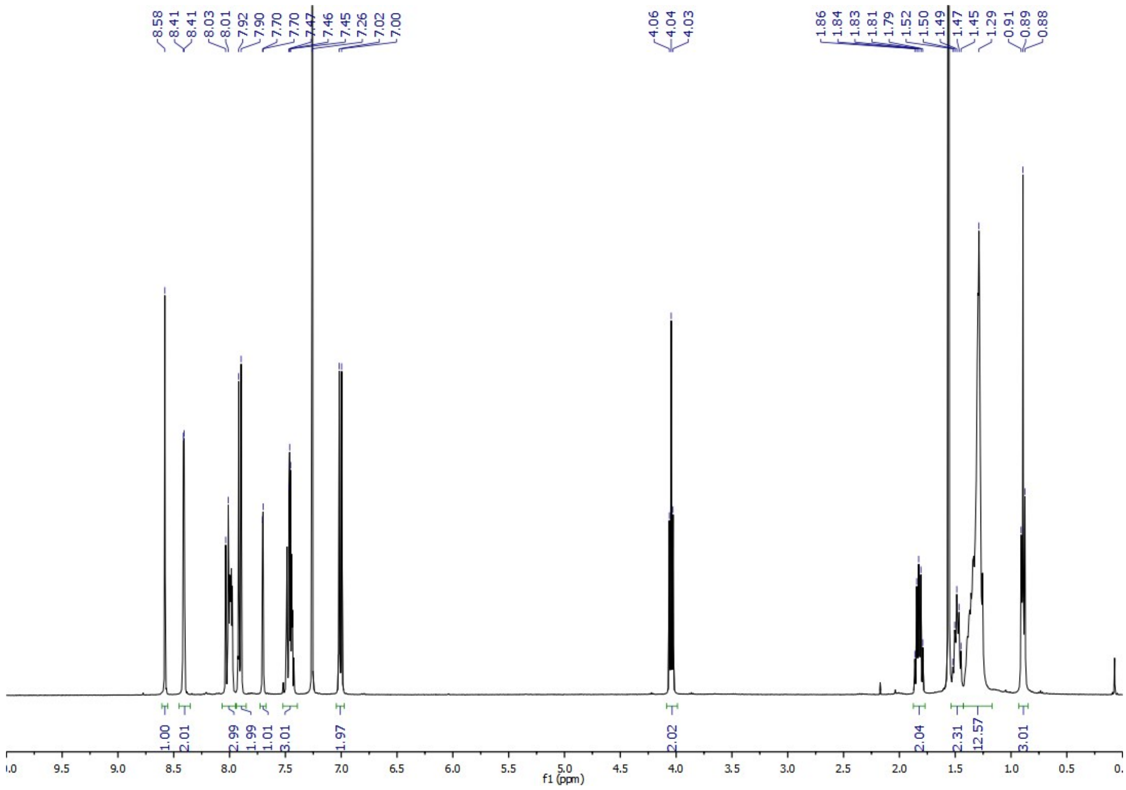

Figure 2(a). [1]H NMR spectrum of 2-[(E)-((4-decyloxyphenyl)methylidene)amino]-anthracene.

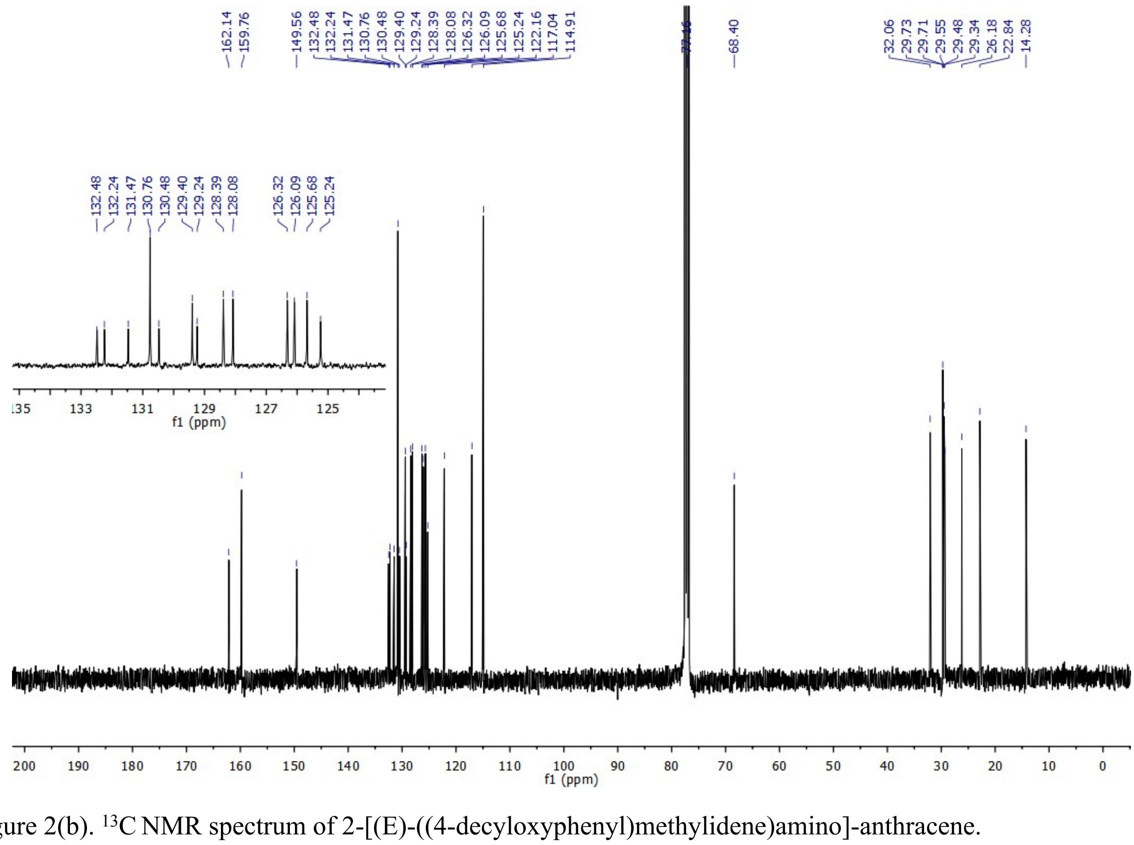

Figure 2(b). [13]C NMR spectrum of 2-[(E)-((4-decyloxyphenyl)methylidene)amino]-anthracene.

[1]H COSY spectrum

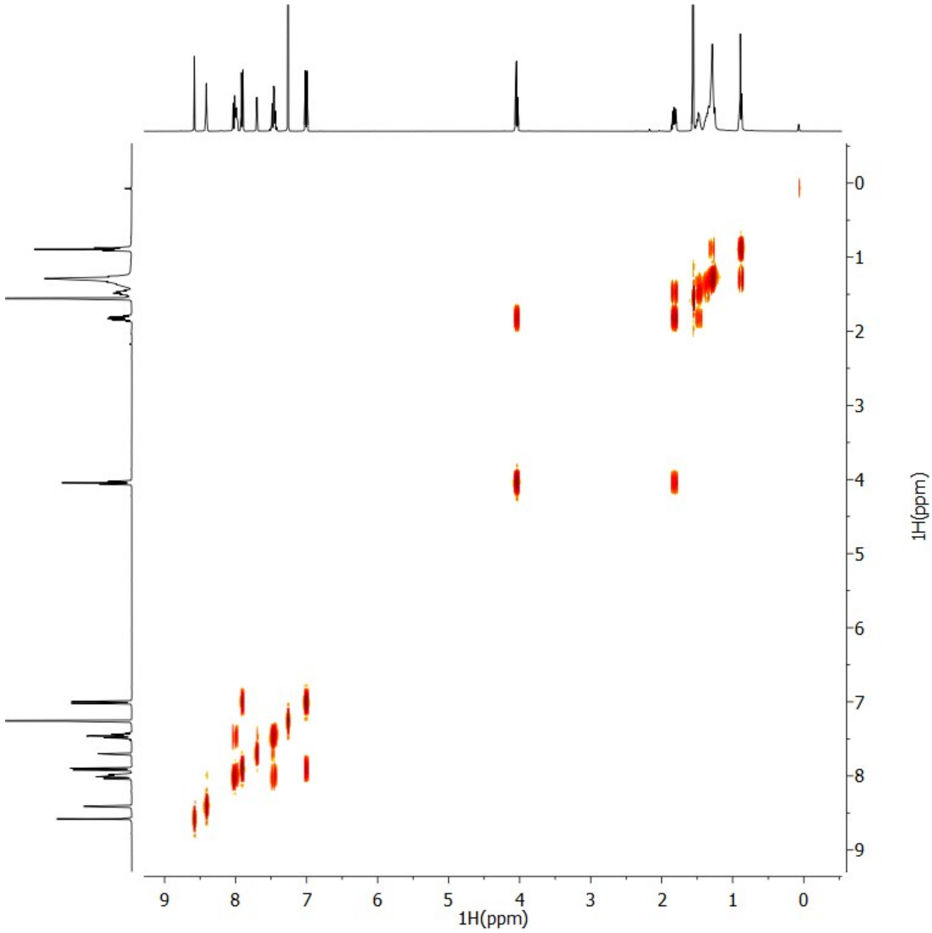

Figure 3. 1H COSY spectrum of 2-[(E)-((4-decyloxyphenyl)methylidene)amino]-anthracene.

Mass spectrum

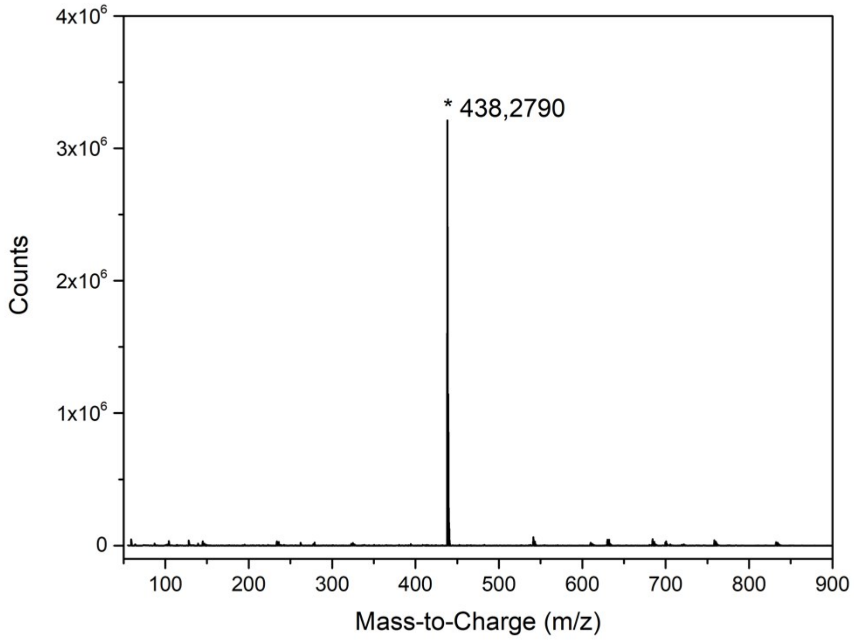

Figure 4. HRMS spectrum of 2-[(E)-((4-decyloxyphenyl)methylidene)amino]-anthracene. Analysis parameters were as follows: Gas temperature (150°C, 5 L/min), Nebulizer (35 psig), Sheath gas (375°C, 12 L/min) Vcap (3500 V), nozzle voltage (2000 V), fragmentor (100 V), skimmer (65 V)
OCT1RFVpp (750 V).

Emission spectrum and fluorescence lifetime

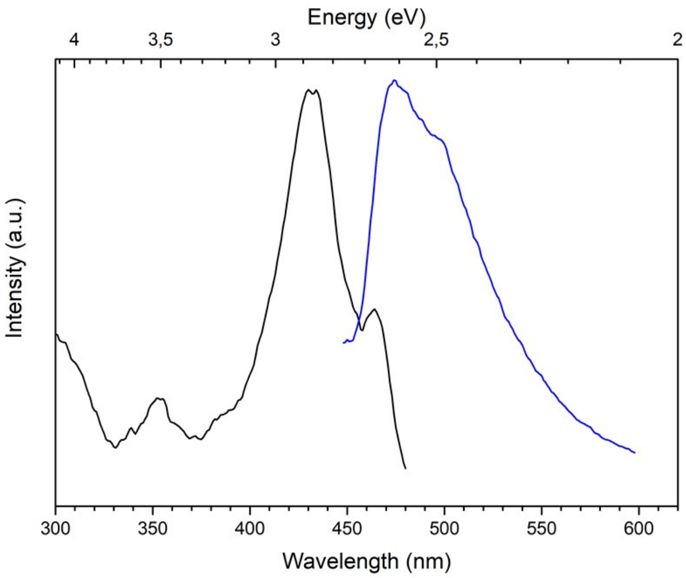

(a)

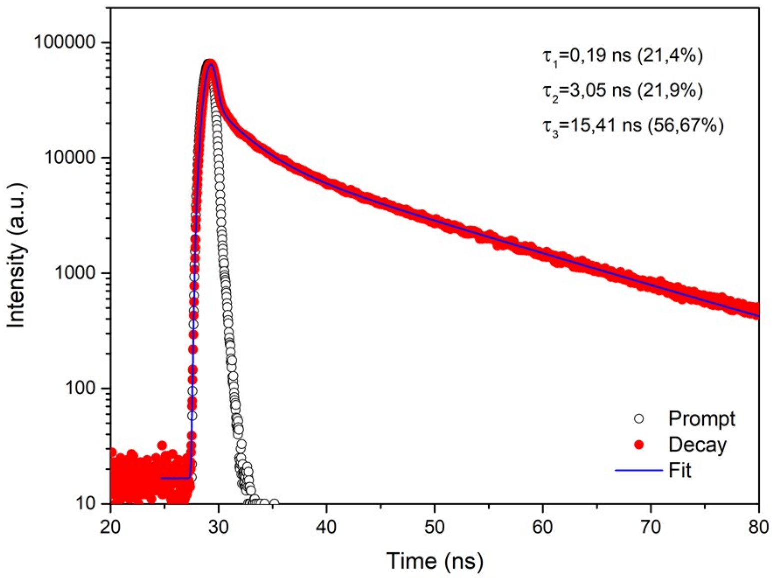

(b)

Figure 5. (a) Excitation (black line, emission wavelength - 480nm) and emission (blue line, excitation wavelength - 435nm) spectrum of 10-OPIA. (b) Fluorescence decay of dilute (10^{-5}M) 10-OPIA solution in acetone. Empty circles: instrument response function. Red circles: experimental data for 10-OPIA solution. Blue line: data fit.

Cyclic voltammograms

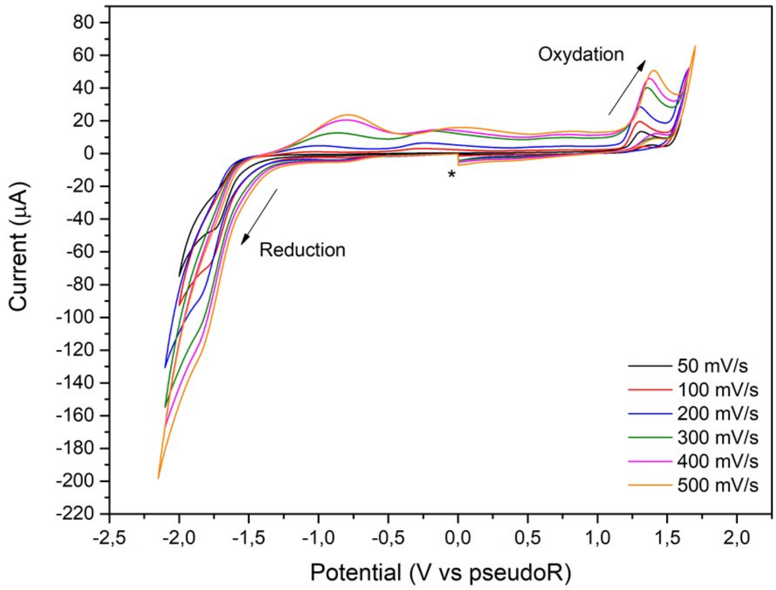

Figure 6. Cyclic voltammetry data of 2mmol 10-OPIA in 0.1M TBAPF6 in DCM, degassed with Ar 20 minutes versus silver wire pseudoreference. Asterisk indicates the start of data collection.

Thermophysical and mesogenic properties

In order to investigate the phase behavior of the10-OPIA material, we have performed calorimetric analysis by DSC. The results (second heating and cooling) are shown in Figure 7. It is clear that 10-OPIA exhibits mesomorphic properties, since the thermogram displays at least 4 phase transitions. Moreover, it is clear that these phase transitions are reversible since they are present on both heating and cooling.

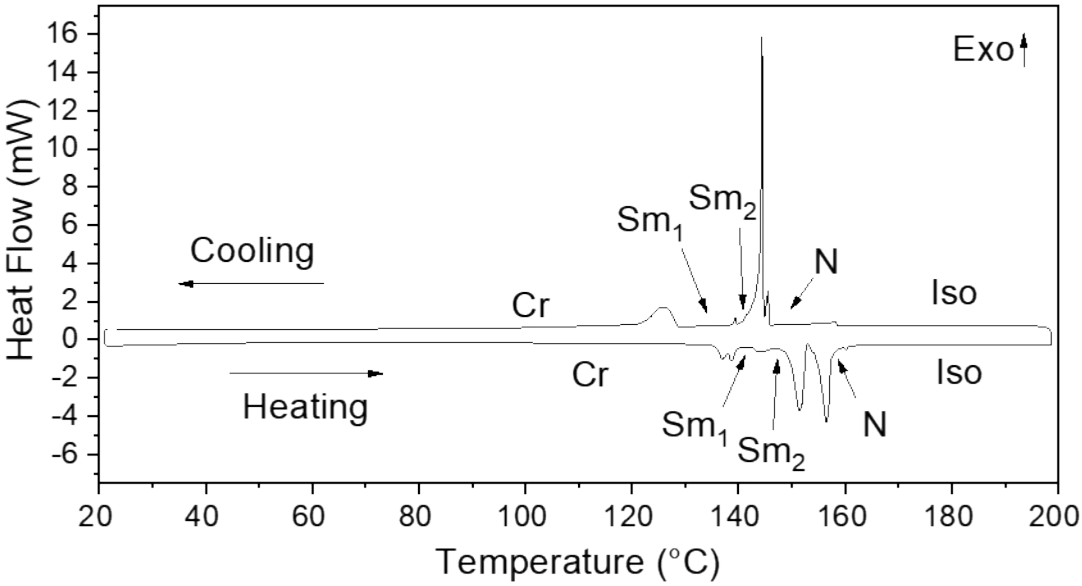

Figure 7. DSC thermograms of 10-OPIAsample obtained on heating and cooling with a rate of 10°C/min.

In order to describe these phase transitions, we are going to proceed from the heating part of the data: the first transition is split in 2 peaks and occurs at 139°C (this splitting is repetitive and may indicate transition to a closely related phase state which appears briefly). It corresponds to melting to the smectic mesophase Sm_1. The second phase transition occurs on 145°C with a relatively low enthalpy change, which may indicate a minor order decrease. This allows us to propose a second smectic phase Sm_2 to this intermediate mesophase, Sm_1 being of higher order than Sm_2. Next phase transition occurs at 152°C with a large enthalpic signature and has a similar two-peak pattern. The high energy of this transition indicates a major order decrease, probably a transformation to a nematic (N) phase from Sm_2. Finally, 10-OPIA completely melts into the isotropic liquid at 160°C. Upon examining the cooling part of the data, one can notice similar phase sequence to that observed on heating, with an exception for the 10-OPIA's tendency of supercooling. The texture of Sm_1 and Sm_2 mesophases look similar to the crystalline phase (polarized microphotographs of cell with homogeneous orientation with a 9 µm spacer filled with 10-OPIA are assembled in Figure 8), which confirms the analysis of the DSC data. The picture taken at 159°C on cooling confirms the homogeneously oriented nematic phase.

Polarized optical microscopy

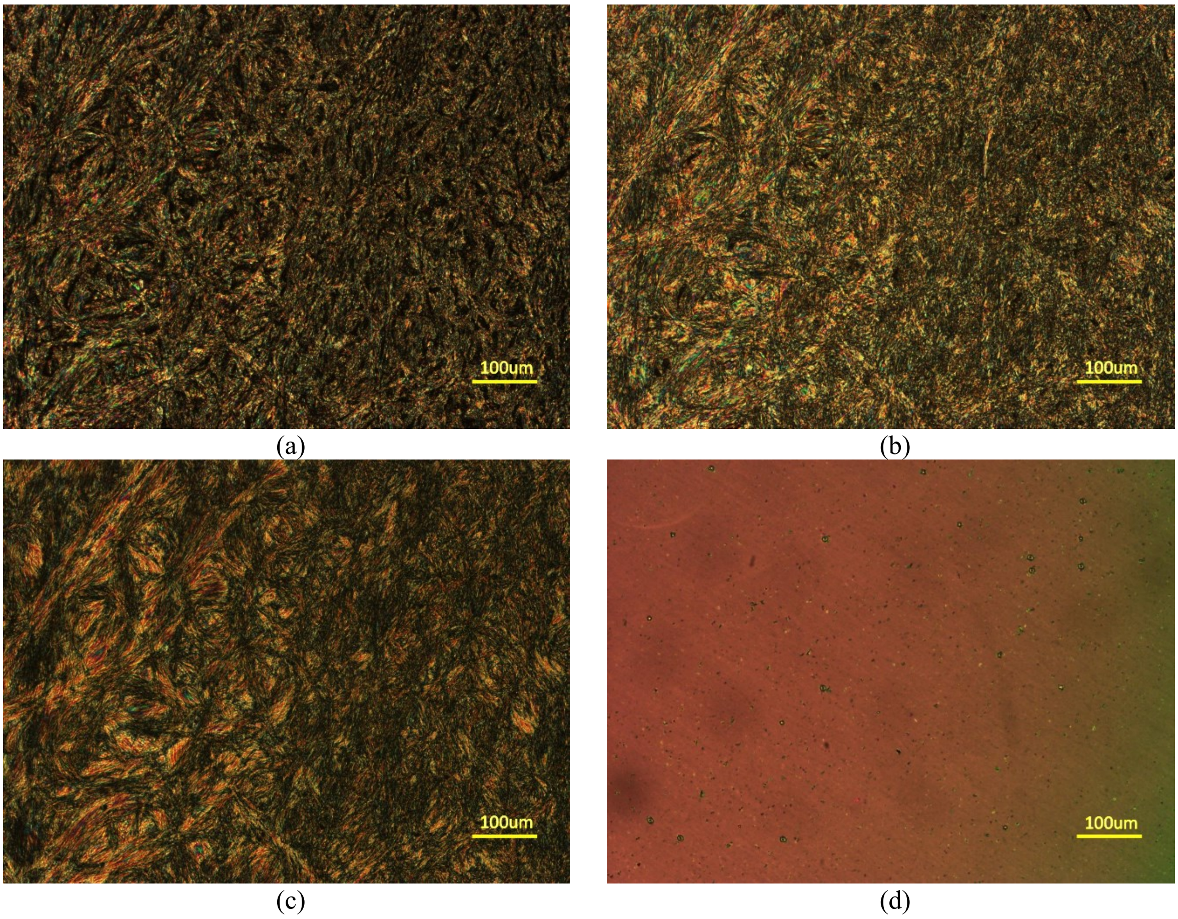

(a) (b) (c) (d)

Figure 8. Sample texture under crossed analyzer-polarizer for pure 10-OPIA (a) in crystalline phase (Cr) at 120°C, (b) Sm1 mesophase at 140°C, Sm2 mesophase at 148°C and nematic (N) mesophase at 159°C.

Drop-casting setup

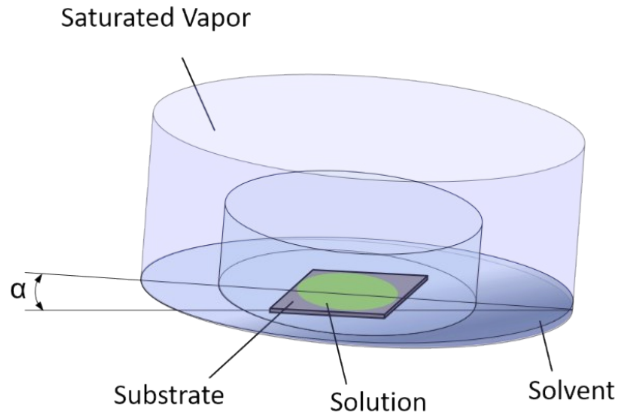

Figure 9. Schematic representation of drop-casting setup. α is the substrate inclination angle.

SEM captures

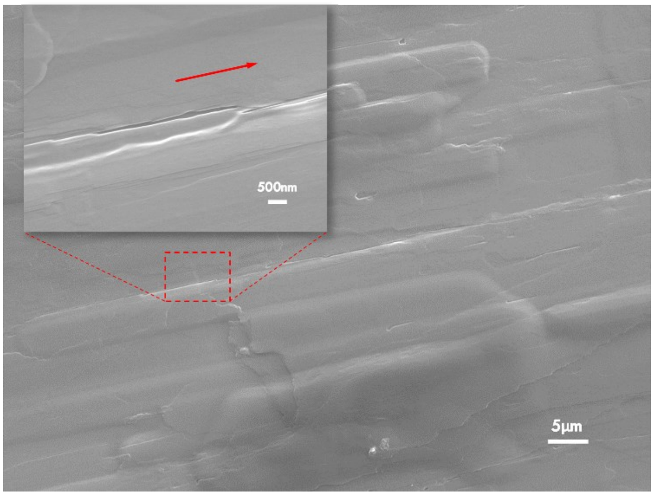

(a)

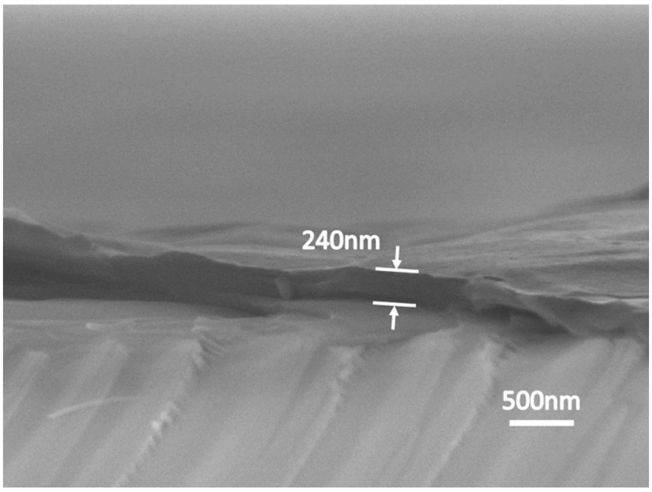

(b)

Figure 10. SEM images of 10-OPIA film prepared by drop-casting of 0.5% wt. solution in chlorobenzene on OTS-18 functionalized glass slide at 3 degree substrate inclination: (a) topography (red arrow indicates direction of crystallization) (b) profile of the same thin film.

AFM topography

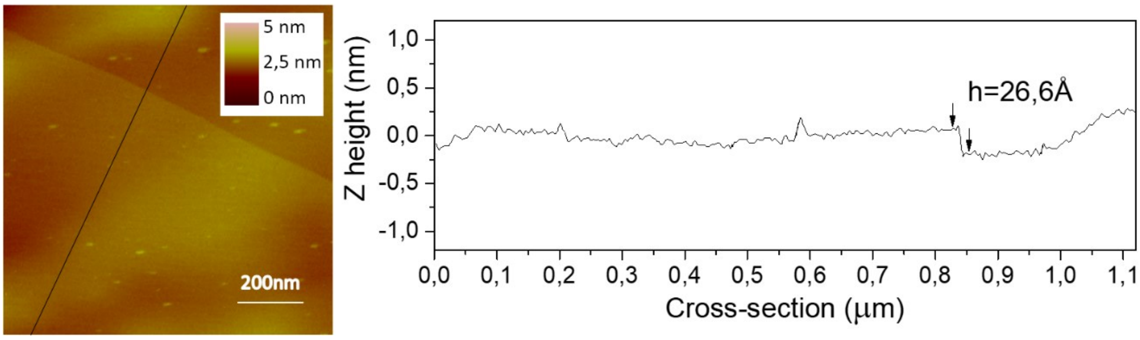

Figure 11. AFM topology (left) and a cross-section (right) of drop-casted 10-OPIA film on OTS-18 functionalized glass slide at 3 degree substrate inclination.

OFET in linear configuration

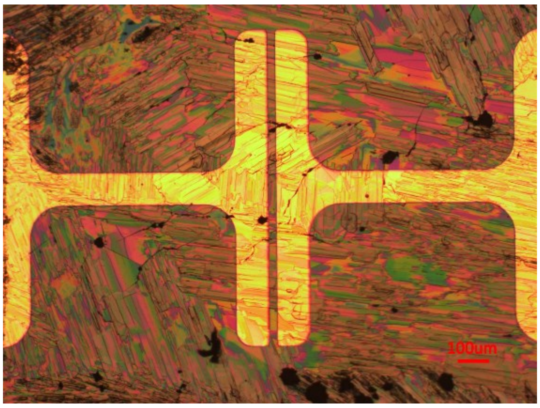

(a)

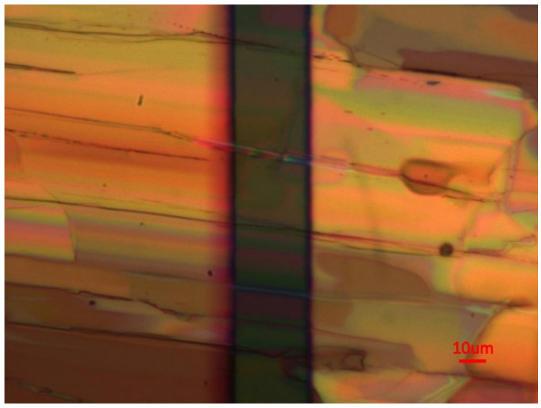

(b)

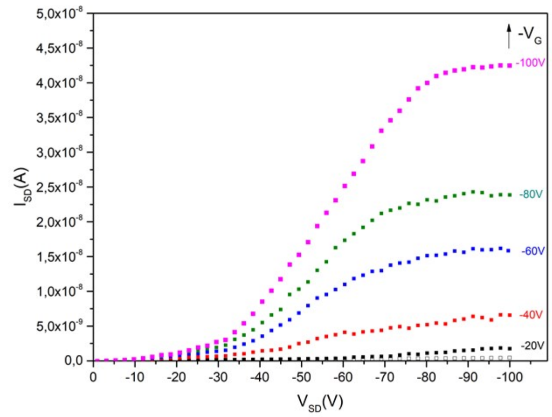

(c)

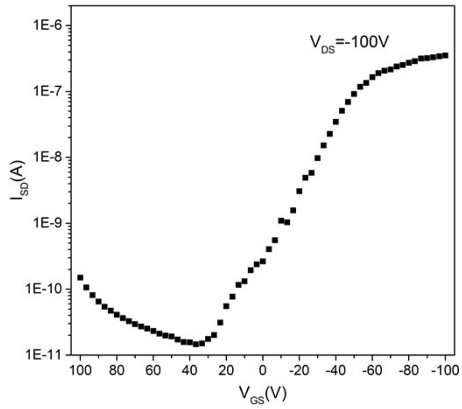

(d)

Figure 12. Microscope captures (in polarized light) with 5x lens (a) and 50x lens (b) of a linear electrode OFET (L = 30 µm, W=1mm) prepared with 10-OPIA, drop-casted, 3 degree substrate inclination. Output (c) and transfer (d) characteristics of this device.

Photocurrent

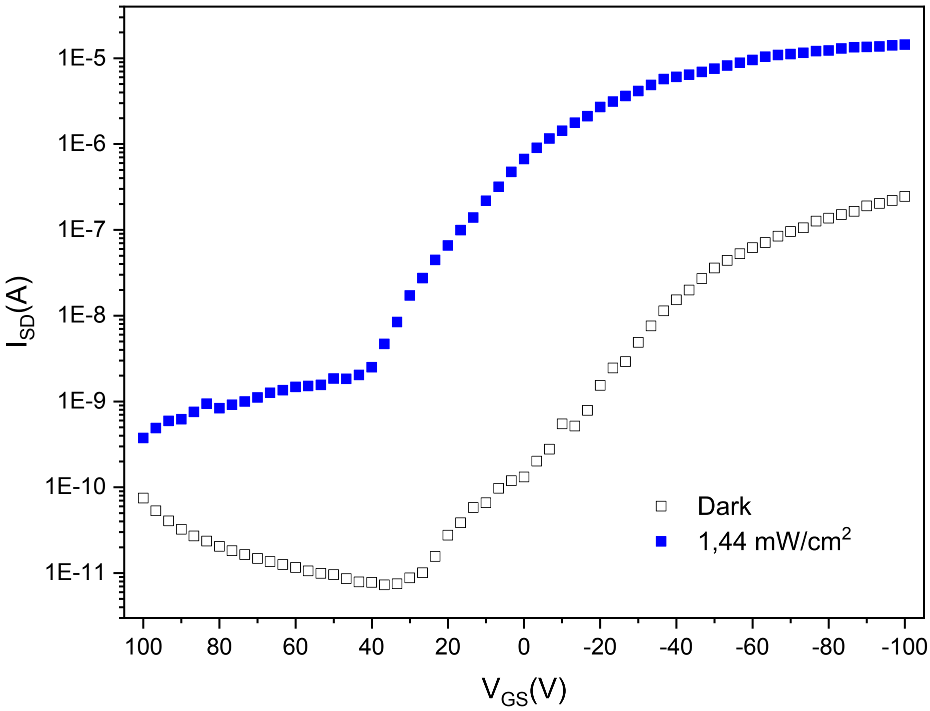

Figure 13. Transfer characteristic of an OFET (L = 50 µm, W=18mm) under illumination (blue symbols) and in the dark (open symbols).

Schemes of photoconductive and photo-gating effects

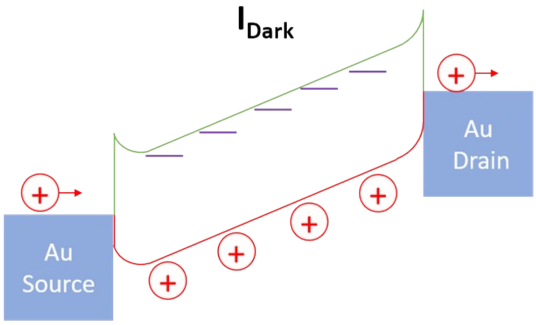

(a)

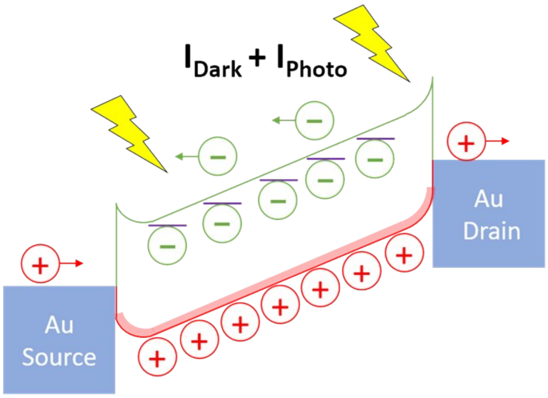

(b)

Figure 14. Energy band (approximation used here for simplicity) diagram for OFET channel (a) in dark conditions and (b) under illumination. Trap states (horizontal bars near the edge of conduction band) and trap filling by minority carriers is shown.